

A new EXAFS method for the local structure analysis of low-Z elements

Noritake Isomura,^{a*} Masao Kamada,^b Takamasa Nonaka,^a Eiken Nakamura,^{b,c} Takumi Takano,^{b,c} Harue Sugiyama^b and Yasuji Kimoto^a

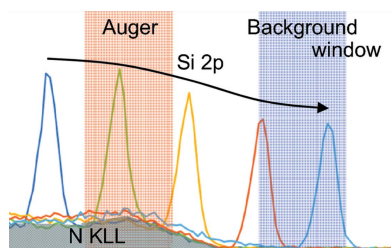
^aToyota Central R&D Laboratories, 41-1 Yokomichi, Nagakute, Aichi 480-1192, Japan, ^bAichi Synchrotron Radiation Center (AichiSR), 250-3 Minamiyamaguchi-cho, Seto, Aichi 489-0965, Japan, and ^cNagoya University Synchrotron Radiation Research Center, Furo-cho, Chikusa-ku, Nagoya, Aichi 464-8603, Japan.
*Correspondence e-mail: isomura@mosk.tytlabs.co.jp

A unique analytical method is proposed for local structure analysis *via* extended X-ray absorption fine structure (EXAFS) spectroscopy. The measurement of electron energy distribution curves at various excitation photon energies using an electron energy analyzer is applied to determine a specific elemental Auger spectrum. To demonstrate the method, the N *K*-edge EXAFS spectra for a silicon nitride film were obtained *via* simultaneous measurement of the N *KLL* Auger and background spectra using dual-energy windows. The background spectrum was then used to remove the photoelectrons and secondary electron mixing in the energy distribution curves. The spectrum obtained following this subtraction procedure represents the 'true' N *K*-edge EXAFS spectrum without the other absorptions that are observed in total electron yield N *K*-edge EXAFS spectra. The first nearest-neighbor distance (N–Si) derived from the extracted N *K*-edge EXAFS oscillation was in good agreement with the value derived from Si *K*-edge analysis. This result confirmed that the present method, referred to as differential electron yield (DEY)-EXAFS, is valid for deriving local surface structure information for low-*Z* elements.

1. Introduction

X-ray photoelectron spectroscopy (XPS) is an extensively used technique in surface science because it can provide not only elemental but also chemical information. However, local atomic structure information is increasingly required for further evaluations. X-ray absorption fine structure (XAFS) spectroscopy provides such information (Stern & Heald, 1983) and is thus expected to be applied in surface science.

Chemical states, such as valence states, can be obtained using X-ray absorption near-edge structure (XANES) spectroscopy (Stöhr, 1992). Furthermore, local structure parameters, such as interatomic distances and coordination numbers, can be derived from extended XAFS (EXAFS) spectra (Teo & Joy, 1980). However, it is difficult to perform EXAFS analyses for low-*Z* elements, because each EXAFS oscillation often overlaps the absorption edge of the next atomic number element. To date, the local structures of these elements have typically been assumed by comparing their spectra with the experimental or calculated XANES spectra of standard samples. Although the partial fluorescence yield (FY) measurement mode may enable EXAFS analysis without the above-mentioned overlap (Eisebitt *et al.*, 1993), surface information cannot be obtained because of the deeper analysis depth (of the order of 100 nm) of partial FY. In addition, although small grazing angle FY measurements do provide surface information (Oyanagi *et al.*, 1995), the sample



surface must be very smooth and FY is not effective for low-*Z* elements because of their small fluorescence yield.

On the other hand, the Auger electron yield (AEY) measurement mode is surface sensitive (Brennan *et al.*, 1981) because it does not detect the secondary electrons originating from deeper depths that are included in the total electron yield (TEY). The Auger peak for a specific element does not include other elemental information, suggesting that AEY analysis may provide an EXAFS spectrum for that specific element. However, photoelectrons cross the Auger peak during incident X-ray energy sweeps, which is a significant problem for EXAFS because of its wide energy range, commonly greater than 400 eV, to perform Fourier transformation of the EXAFS oscillation. This is not an issue for XANES, which has a narrow energy range. Auger peaks have specific kinetic energies (hereafter referred to as ‘electron energies’ to distinguish them from X-ray energies), and the photoelectron peaks are shifted during an X-ray energy sweep. In conventional AEY mode, which observes the intensity of an Auger peak at a fixed electron energy, the intensity increases in the narrow energy region where the photoelectron peaks cross, resulting in the modification of the EXAFS spectrum. Herein, we propose a new method for avoiding this increase in intensity because of photoelectrons by simultaneously monitoring the intensities of the Auger and background spectra (at electron energies higher than those of the Auger peak) using dual-energy windows and an electron energy analyzer. The EXAFS spectrum is then generated by subtracting the background intensity from the obtained electron energy distribution curves (EDCs) to provide the ‘true’ specific absorption edge EXAFS spectrum that is not affected by photoelectron crossing or other absorption edges. Hence, the present method, referred to as differential electron yield (DEY)-EXAFS, is effective for the EXAFS analysis of low-*Z* elements on material surfaces. In this study, the potential of the new method for the N *K*-edge EXAFS analysis of a well defined sample (silicon nitride) has been demonstrated.

2. Experimental

Experiments were performed at the vacuum ultraviolet and soft X-ray XAFS and angle-resolved photoelectron spectroscopy beamline BL7U of the Aichi Synchrotron Radiation Center (AichiSR), which has an electron storage ring with a circumference of 72 m and is operated at an electron energy of 1.2 GeV with a current of 300 mA.

Quasi-monochromatic light from an undulator was monochromated using a variable-included-angle Monk–Gillieson mounting monochromator with a varied-line-spacing plane grating. Through a combination of undulator radiation and sophisticated monochromator design (variable-included-angle mechanism) and using two gratings, the monochromator can cover the photon energy range of 30–850 eV with a resolving power of greater than 3000 at 200 eV. The beam size at the sample position was 0.4 mm (h) × 0.1 mm (v). The horizontal size of the irradiated region of the sample surface depended on the sample tilt.

The electron energy analyzer (MBS A-1, MB SCIENTIFIC AB) was effective over a range of kinetic energies (up to 12 keV) and comprised a hemispherical energy analyzer with a mean radius of 200 mm, a pre-retarding combined second-order focusing lens system, and a two-dimensional event-counting detector equipped with a microchannel plate, a phosphor screen, and a charge-coupled device camera. The entrance slit of the analyzer was rectangular with dimensions of 0.8 mm in the energy-dispersive direction and 25 mm in the energy-nondispersive direction. The pass energy was 100 eV. The analyzer input lens axis, with an acceptance angle of ±18°, was aligned 45° to the incident X-ray beam and parallel to the polarization vector. The take-off angle of the analyzed electrons was set to 90° (normal to the surface). The total bandwidth of the present measurement was approximately 0.36 eV at the N *K*-edge. The base pressure of the main chamber was approximately 5×10^{-9} Pa.

The sample was a silicon nitride film on a Si substrate. The film was deposited *via* low-pressure chemical vapor deposition at 1273 K using SiH₂Cl₂ and NH₃ as the source gases. The film thickness was greater than 100 nm.

3. Results and discussion

Fig. 1 shows the XPS spectrum for the silicon nitride surface at a photon energy of 600 eV. The Auger and photoelectron peaks of the constituent elements are observed. In addition, C 1s and O 1s photoelectron peaks caused by contaminants can also be seen. In general, the spectral background increases at lower photoelectron peak energies because of inelastic electrons that originate from deeper depths; therefore, elements attached to the sample surface do not produce such background increases (Briggs & Rivière, 1983).

Fig. 2 shows the EDCs obtained at photon energies of 473, 481, 489, 497 and 505 eV. The N *KLL* Auger peaks can be seen over the range of 360–385 eV. The five photoelectron peaks, each with a full width at half-maximum (FWHM) of approximately 3 eV, are all attributed to Si 2*p* and were observed to move to higher electron energies and cross the Auger peak as the photon energy increased. The Auger and background intensities were monitored as the integrations

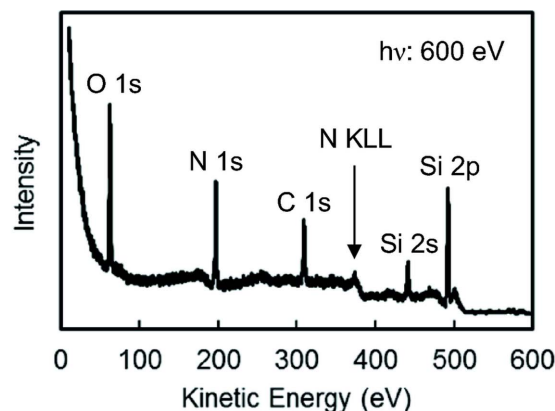


Figure 1 XPS spectrum of the silicon nitride surface at a photon energy of 600 eV.

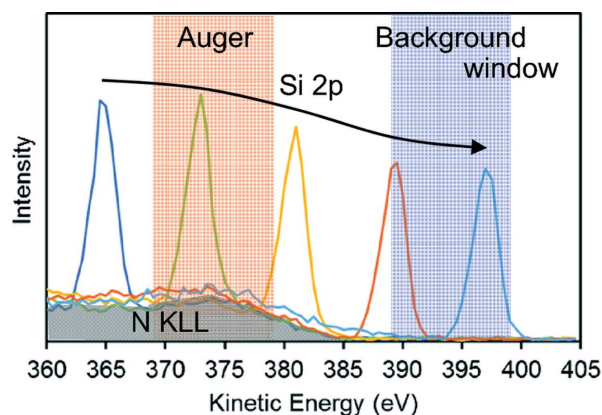


Figure 2

EDCs at photon energies of 473, 481, 489, 497 and 505 eV, indicated as blue, green, yellow, red and light-blue lines, respectively. The gray area indicates the N *KLL* Auger peak. The red and blue areas indicate the energy windows, and their integrated intensities were used to derive the EXAFS spectra. The five photoelectron peaks are attributed to Si *2p* and moved to higher kinetic electron energies as the photon energy increased.

within the electron energy windows from 369–379 eV and 389–399 eV, respectively, during X-ray energy sweeps for the EXAFS measurements (hereafter referred to as the ‘Auger EXAFS’ and ‘background EXAFS’, respectively).

The N *K*-edge Auger and background EXAFS spectra are shown in Fig. 3. The intensities were normalized by the incident X-ray intensities, which were determined using the photoelectron yield of an Au mesh placed between the final mirror and the sample. As can be seen in Fig. 3, the N *K*-edge was observed in the Auger EXAFS spectrum, but not in the background spectrum. However, the spectral shapes other than for the N *K*-edge were quite similar. In both spectra, several local intensity increases because of photoelectron crossing, each with an energy width of 10 eV, were presented (indicated by the brackets in Fig. 3). The rising and falling edges of those increases were not abrupt, and their centers were nearly flat, because the photoelectron peaks that crossed with electron energy windows of 10 eV had Gaussian-like shapes with FWHMs of 3 eV, as observed in Fig. 2. In addition,

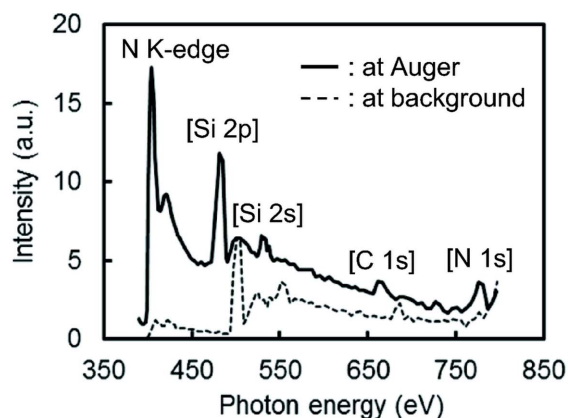


Figure 3

N *K*-edge EXAFS spectra measured at different N *KLL* Auger peaks (369–379 eV) and backgrounds (389–399 eV). The brackets indicate the intensity increases because of photoelectrons crossing electron energy windows for the Auger and background spectra.

the background EXAFS spectrum was shifted to a higher energy than the Auger EXAFS spectrum (by 20 eV) because the energy window for the background was placed at an electron energy 20 eV higher than that of the Auger, and the photoelectron peaks crossed each energy window at photon energies that differed by 20 eV.

There is apprehension that resonant excitation of higher-energy edges (the O-*K* in this study) could have an effect on the intensity of the N *KLL* Auger, which is the source of the Auger EXAFS spectrum. One possibility is the reduction of the number of photons available for excitation of N. This reduction is due to the photons being used for excitation of O when the photon energy is tuned to the O *K*-edge resonance. No local intensity reduction was observed at the photon energy of the O *K*-edge in the background EXAFS spectrum in Fig. 3, and also the Si *2s* photoelectron intensity did not reduce when it crossed the monitoring window of the EDCs (no data shown). These results suggest no reduction in the number of photons. Another possibility is that of multiple atom resonant photoemission (MARPE). Kay *et al.* reported that a significant enhancement was observed in the core-level photoelectron and Auger peak intensities associated with one element in the sample when the excitation energy was tuned through an energetically deeper absorption edge of a second element in metal oxides (Kay *et al.*, 1999; Arenholz *et al.*, 2000). As shown in Fig. 3, no local intensity increase was observed at the photon energy of the O *K*-edge in the N *K*-edge Auger EXAFS spectrum, although it is difficult to discriminate because another local intensity increase due to the Si *2s* photoelectron crossing is present nearby, suggesting little or no effect of MARPE. In the case of oxide samples, these effects of resonant excitation of higher-energy edges might have to be considered.

The N *K*-edge DEY-EXAFS spectrum obtained by following subtraction of the background spectrum from the EXAFS spectrum is shown in Fig. 4, along with the TEY-EXAFS spectrum for comparison. The subtraction was performed after shifting the background EXAFS spectrum by 20 eV to a lower energy. In addition to the N *K*-edge at 405 eV, local maxima at 420 and 480 eV, likely because of EXAFS oscillations, were observed in the DEY-EXAFS spectrum. Although it is possible that the additional oscillations except for the local intensity increases may be caused by crossing photoelectrons, such as Si *2p*, Si *2s* and C *1s* shown in Fig. 3, it is assumed that the elastic photoelectron intensity would not exhibit the same modulations as the absorption coefficient (Stöhr *et al.*, 1984; Lee, 1976). In the TEY-EXAFS spectrum, in addition to the N *K*-edge, the O *K*-edge was also observed at 540 eV. The presence of another absorption edge, such as the O *K*-edge, in addition to the N *K*-edge, would make the EXAFS analysis impossible. Notably, the DEY-EXAFS spectrum obtained in the present study does not include the O *K*-edge, as shown in Fig. 4.

Fig. 5 presents the DEY-EXAFS and TEY-EXAFS oscillations for the N *K*-edge extracted from each EXAFS spectrum using the *ATHENA* program (Ravel & Newville, 2005) as a function of the wavevector. The TEY oscillation includes

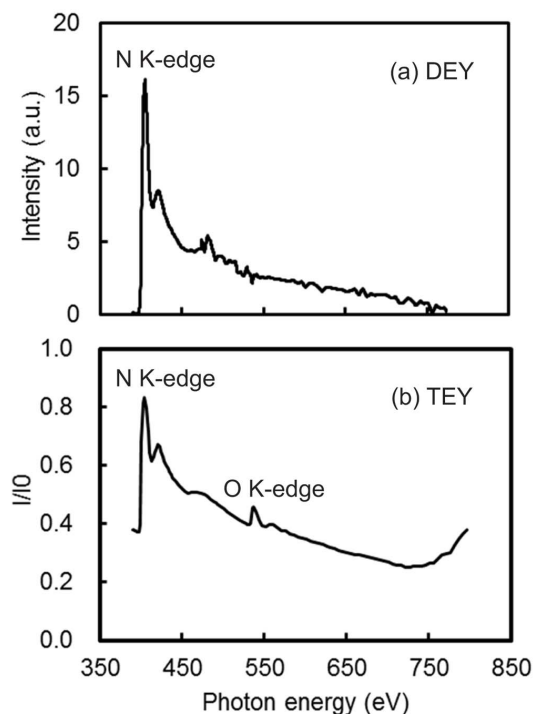


Figure 4
(a) DEY-EXAFS and (b) TEY-EXAFS spectra for the N *K*-edge.

the O *K*-edge with a *k* value of greater than 6 Å⁻¹. The DEY-EXAFS oscillation is nearly the same as the TEY oscillation with a value for *k* of at least less than 6 Å⁻¹ without the O *K*-edge. This result indicates that the present new method is valid.

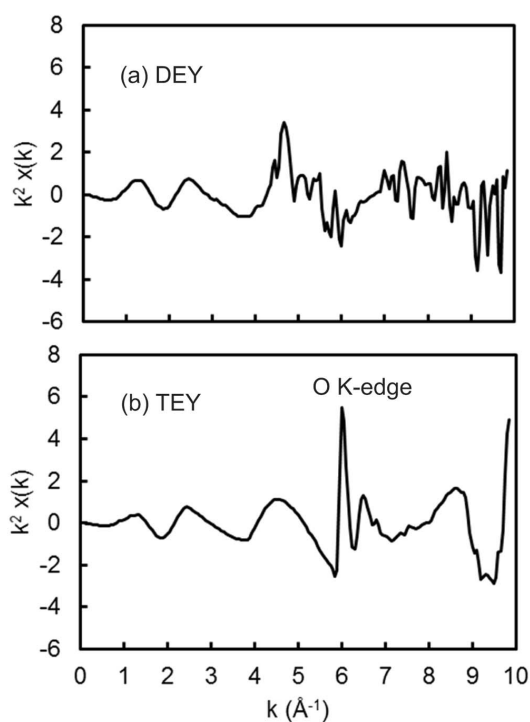


Figure 5
(a) DEY-EXAFS and (b) TEY-EXAFS oscillations for the N *K*-edge as a function of the wavevectors from Fig. 4.

Fig. 6 shows the Fourier transforms, without consideration of phase shifts, derived from the oscillations of the N *K*-edge DEY-EXAFS and the Si-*K* TEY-EXAFS for comparison. For the N *K*-edge, the oscillation range used for the Fourier transform was $k = 2.6\text{--}7.8 \text{ \AA}^{-1}$ with a relatively good signal-to-noise ratio, and the phase shift and backward scattering factor values were calculated using *FEFF* (Zabinsky *et al.*, 1995; Ankudinov *et al.*, 1998). The Si *K*-edge was measured at the BL6N1 beamline of AichiSR (Yamamoto *et al.*, 2014; Isomura *et al.*, 2015), and the obtained TEY-EXAFS spectrum included no other edge (no data shown), enabling EXAFS analysis. The first nearest-neighbor distances were calculated *via* a fitting analysis using the *ARTEMIS* program (Ravel & Newville, 2005). The parameters included the atomic distance, amplitude and edge energy, and the Debye–Waller factor was fixed. The N–Si distances obtained from the N and Si *K*-edges were 1.69 and 1.70 Å with reliability factors (*R* factors) of 0.013 and 0.046, respectively, showing good agreement. Stöhr (1979) performed N *K*-edge TEY-EXAFS measurements for a similar silicon nitride film without surface contamination (after surface cleaning *via* ion sputtering) and reported an N–Si distance of 1.71 Å, which is in close agreement with the value obtained in the present study (1.69 Å). These results indicate that the N–Si distance on the natural surface of silicon nitride stored under standard conditions for one week after crystal growth may be nearly the same as that in bulk silicon nitride.

On the basis of these results, it can be concluded that the ‘true’ N *K*-edge EXAFS spectrum without other absorption edges, which is surface sensitive, was obtained using the proposed DEY-EXAFS method.

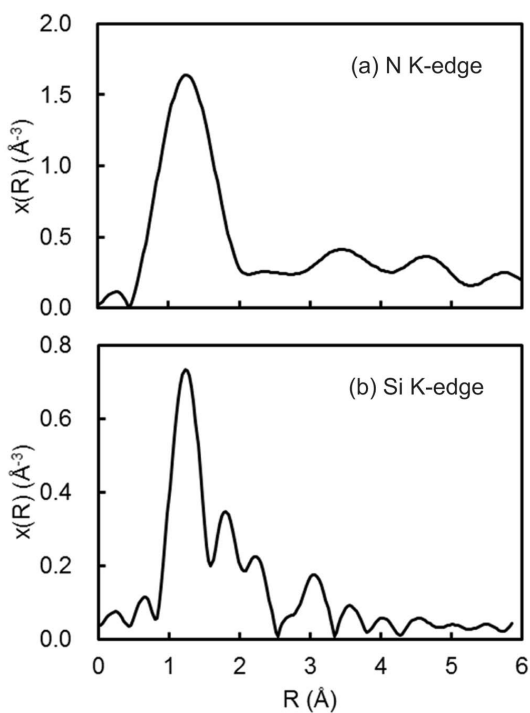


Figure 6
Fourier transforms derived from the EXAFS oscillations for the (a) N *K*-edge and (b) Si *K*-edge, without consideration of phase shifts.

4. Conclusions

A unique local structure analysis method for low-*Z* elements using electron energy distribution curves was proposed in which the obtained EXAFS spectrum includes no other absorption edges within the EXAFS oscillation. The measurements were performed by simultaneously monitoring the intensities of the Auger electron and background EDC with dual-energy windows using an electron energy analyzer. The background spectrum was used to remove intensity increases because of photoelectron crossing of the Auger peak. The resultant differential spectrum represents the ‘true’ specific absorption edge EXAFS spectrum with no other edges. The method is referred to as differential electron yield (DEY)-EXAFS. The N *K*-edge DEY-EXAFS spectrum for a silicon nitride film was obtained using this proposed method. The Fourier transformation was derived from the extracted EXAFS oscillation. The obtained first nearest-neighbor distance (N–Si) was in good agreement with the value derived from the Si *K*-edge and close to the previously reported value. This result demonstrates that the obtained N *K*-edge DEY-EXAFS spectrum is valid for surface analysis and also suggests that the N–Si distance on the natural surface of silicon nitride may be nearly the same as that in bulk silicon nitride. The proposed DEY-EXAFS method should pave the way for local structure analysis of low-*Z* elements, particularly on sample surfaces. Moreover, it does not require smooth sample surfaces and should also be applicable for rough surfaces.

Acknowledgements

The authors are grateful to Dr Hirozumi Azuma and Dr Yoshio Watanabe of AichiSR for their continual encouragement and support. The synchrotron radiation measurements

were performed at BL7U of AichiSR, Aichi Science & Technology Foundation, Aichi, Japan (Experimental Nos. 201405062 and 201406058).

References

- Ankudinov, A. L., Ravel, B., Rehr, J. J. & Conradson, S. D. (1998). *Phys. Rev. B*, **58**, 7565–7576.
- Arenholz, E., Kay, A. W., Fadley, C. S., Grush, M. M., Callcott, T. A., Ederer, D. L., Heske, C. & Hussain, Z. (2000). *Phys. Rev. B*, **61**, 7183–7186.
- Brennan, S., Stöhr, J. & Jaeger, R. (1981). *Phys. Rev. B*, **24**, 4871–4874.
- Briggs, D. & Rivière, J. C. (1983). *Practical Surface Analysis*, edited by D. Briggs and M. P. Seah, p. 181. Chichester: John Wiley and Sons.
- Eisebitt, S., Rubensson, J.-E., Böske, T. & Eberhardt, W. (1993). *Phys. Rev. B*, **48**, 17388–17392.
- Isomura, N., Soejima, N., Iwasaki, S., Nomoto, T., Murai, T. & Kimoto, Y. (2015). *Appl. Surf. Sci.* **355**, 268–271.
- Kay, A. W., Arenholz, E., Mun, B. S., Garcia de Abajo, J., Fadley, C. S., Denecke, R., Hussain, Z. & Van Hove, M. A. (1999). *J. Electron Spectrosc. Relat. Phenom.* **101–103**, 647–652.
- Lee, P. A. (1976). *Phys. Rev. B*, **13**, 5261–5270.
- Oyanagi, H., Shioda, R., Kuwahara, Y. & Haga, K. (1995). *J. Synchrotron Rad.* **2**, 99–105.
- Ravel, B. & Newville, M. (2005). *J. Synchrotron Rad.* **12**, 537–541.
- Stern, E. A. & Heald, S. M. (1983). *Handbook on Synchrotron Radiation*, Vol. 1b, edited by E. E. Koch, p. 955. Amsterdam: North-Holland.
- Stöhr, J. (1979). *J. Vac. Sci. Technol.* **16**, 37.
- Stöhr, J. (1992). *NEXAFS Spectroscopy*, Springer Series in Surface Science, Vol. 25. Berlin: Springer-Verlag.
- Stöhr, J., Noguera, C. & Kendelewicz, T. (1984). *Phys. Rev. B*, **30**, 5571–5579.
- Teo, B. K. & Joy, D. C. (1980). *EXAFS Spectroscopy*. New York: Plenum.
- Yamamoto, M., Yoshida, T., Yamamoto, N., Yoshida, H. & Yagi, S. (2014). *e-J. Surf. Sci. Nanotech.* **12**, 299–303.
- Zabinsky, S. I., Rehr, J. J., Ankudinov, A., Albers, R. C. & Eller, M. J. (1995). *Phys. Rev. B*, **52**, 2995–3009.